Acceleration demands on nonstructural components in special concentrically braced frame structures

Neda Salari[1], Vahid Mohsenzadeh[1], Dimitrios Konstantinidis[2], Lydell Wiebe[3]

[1] Ph.D. Candidate, Department of Civil Engineering, McMaster University, Hamilton, Canada.
[2] Assistant Professor, Department of Civil and Environmental Engineering, University of California, Berkeley, USA.
[3] Associate Professor, Department of Civil Engineering, McMaster University, Hamilton, Canada.

ABSTRACT

In several recent earthquakes that struck countries with well-developed seismic codes, the economic losses associated with damage to nonstructural components (NSCs), also known as operational and functional components in Canada, surpassed those due to structural damage. It has been suggested that the reason is twofold: (a) nonstructural components account for a significant portion of the total investment in buildings, and (b) while the seismic design of structural systems has evolved significantly over the past several decades, nonstructural components are either not designed for seismic loads at all, or they are designed using existing code provisions, which are based in most cases on past empirical observations and engineering judgement rather than experimental and analytical research. This investigation focuses on quantifying acceleration demands on nonstructural components in Special Concentrically Braced Frame (SCBF) structures. Two 6-storey SCBF structures are considered (two-storey X and chevron archetypes). Detailed models of the structures are developed in OpenSees, and nonlinear time history analyses are carried out using a suite of 44 far-field ground motions to compute the absolute acceleration response at the different floor levels. The study evaluates the current code formula for seismic design of acceleration-sensitive nonstructural components, which assumes a linear relationship between the ratio of peak floor acceleration to peak ground acceleration (PFA/PGA) and the normalized elevation of the component in the building with respect to the roof height (z/h). The results of the analyses show that improved formulas can be obtained by using a nonlinear relationship between PFA/PGA and z/h. The study also investigates the effect of the dynamic amplification in acceleration-sensitive nonstructural components through evaluation of the generated floor spectra for different levels of damping.

Keywords: Nonstructural Components, Special Concentrically Braced Frame, Seismic Design Force, Acceleration-sensitive, Peak Floor Acceleration

INTRODUCTION

In major seismic events, serious damage to acceleration-sensitive nonstructural components (NSCs) has resulted in significant economic losses and interruption of building functionality. The cost of NSCs may account for 65%–85% of the total construction cost of commercial buildings [1]. Therefore, it is important to ensure that NSCs attached to structures can resist the forces generated during earthquakes. Considering that this is not typically done, it is not surprising that in many post-earthquake reports, losses associated with damage to NSCs have exceeded losses due to structural damage [1, 2]. To improve their seismic performance, extensive research has been aimed at enhancing simplified design procedures for attached NSCs [3-5].

An important step in evaluating or designing acceleration-sensitive NSCs is to quantify the peak floor acceleration (PFA) along the height of the building. The ASCE 7-16 [6] and NBC 2015 [7] provisions for the design force of NSC are based on an empirical relationship that assumes that PFA varies linearly from the Peak Ground Acceleration (PGA) at the ground level to three times the PGA at the roof. As an alternative, Fathali and Lizundia [8] proposed a power-law-type variation, based on observations on PFAs recorded under 16 seismic events in 150 instrumented buildings in California. However, the effect of the lateral load-resisting system was neglected in this empirical equation. Due to the scarcity of previous research on the subject, it is not clear to what degree the actual force demands on NSC vary from the ASCE 7 design force, depending on the characteristics of the lateral load-resisting system. Although the effect of the predominant period of the building on the distribution of PFA was considered by Kehoe and Freeman [9] and Searer and Freeman [10], the results were obtained while the structures remained elastic or only experienced limited nonlinearity. Therefore, better understanding of the seismic demands on NSCs is needed, especially when the structure behaves in the inelastic range.

This paper summarizes the results of a numerical study on the seismic response of two six-storey special concentrically braced frame (SCBF) archetype structures: one featuring chevron bracing and the other two-storey X bracing. The study aims

to provide better insight on the performance of nonstructural components in midrise buildings. Nonlinear response history analyses are conducted for a suite of 44 ground motions, scaled to two different seismic excitation intensities. Results for the variation of PFA/PGA with height are compared with the empirical linear relationship recommended by ASCE 7-16 [6]. Finally, floor spectra are developed and used to quantify the acceleration demands and component amplification factors for attached NSCs.

DESCRIPTION OF ARCHETYPE BUILDINGS

The plan and elevation of the six-storey archetype building considered in this study are the same as one of the buildings considered in the NIST GCR 10-917-8 report [11]. The building has 9.144 m spans in each direction, and the storey height is 4.572 m. The building is designed for an office occupancy (Risk category II and importance factor $I = 1$) and located in San Francisco with site coordinates (37.783°N, 122.392°W), soil class D and Seismic Design Category D_{max} [16]. The corresponding mapped spectral accelerations at 0.2 s and 1 s are $S_S = 1.5$ g and $S_1 = 0.6$ g, respectively. As can be seen in Figure 1 (a), the building has a rectangular plan with two one-bay SCBFs in each direction. Two configurations are considered for the SCBFs: a chevron and a two-storey X, shown in Figure 1 (b) and (c), respectively. The SCBFs are designed in accordance with ANSI/AISC 341-16 [12], ANSI/AISC 360-16 [13], and ASCE/SEI 7-16 [6].
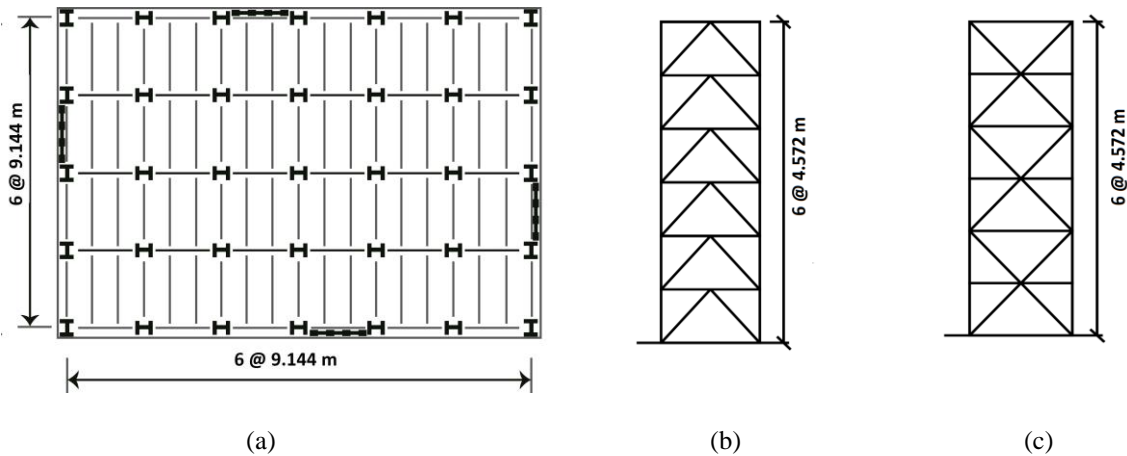

| (a) | (b) | (c) |

Figure 1. Plan and elevation views of the two archetype SCBF structures

Special Concentrically Braced Frames

The SCBF systems are designed with a response modification factor of $R = 6$. The columns are fixed at the base and oriented to bend about the strong axis. The braces consist of circular HSS with slenderness and width-to-thickness ratios that satisfy the ANSI/AISC 341-16 [12] provision for seismically compact sections. The drift ratio limit is 2% for the buildings. Frame members and braces are assumed to have characteristic yield strengths of 345 and 318 MPa, respectively. A dead load of 4.0 kPa and 3.2 kPa and live load of 2.4 kPa and 0.96 kPa are applied on the floor and roof, respectively.

Modeling Assumptions

2D models of the two braced systems were developed in OpenSees [14]. Force-based beam-column elements were used to model the beams, columns, and braces. All beam to column connections were modelled as fixed. The Steel02 material model with 3% strain hardening was used for all elements. To account for P-Δ effects, half of the gravity load of the building was applied to a leaning column that was pinned at the base, and the PDelta geometric transformation formulation was used. The moment of inertia, plastic moment, and the stiffness of one gravity column were multiplied by the number of gravity columns in the tributary area and applied to the leaning column, which was modelled as continuous. The mass of the tributary area of the gravity columns was applied at the nodes of the leaning column.

In order to model the buckling behaviour of the braces, sixteen force-based nonlinear beam–column elements with fibre sections were used with corotational coordinate transformation [15]. A sinusoidal initial out-of-straightness of 0.1% of the brace length at the middle of the brace was applied to trigger buckling. The gusset plates were modeled using fibre beam-

column elements with three integration points. Tangent stiffness-proportional Rayleigh damping of 3% in the first and third modes was used. Table 1 lists the periods of the first four lateral modes of the two SCBF system configurations.

Table 1. Periods of the first four lateral modes

Mode #	Chevron (s)	Two-storey X (s)
1	0.92	0.99
2	0.32	0.37
3	0.26	0.28
4	0.19	0.23

Ground Motions Selection and Scaling

This study uses the FEMA P-695 [16] suite of 22 pairs of far-field ground motion records. Each pair is considered as two independent records (i.e. 44 records total) and scaled to the maximum considered earthquake (MCE) target spectrum using the procedure described in ASCE 7-16 [6]. In this approach, each record is scaled to achieve the minimum mean squared error of the difference between the target spectrum and the record response spectrum. The period range was between $0.2T$ and $2T$, where T corresponded to the fundamental period of the chevron system for the lower limit and that of two-storey X system for the upper limit. In order to obtain the scale factors under the design basis earthquake (DBE), the corresponding MCE scale factors were multiplied by a factor of 2/3. Figure 2 shows the mean 5% damped spectrum of the 44 ground motions matched with the MCE spectrum. The vertical solid and dashed lines indicate the periods of first five modes for the chevron and two-storey X systems.
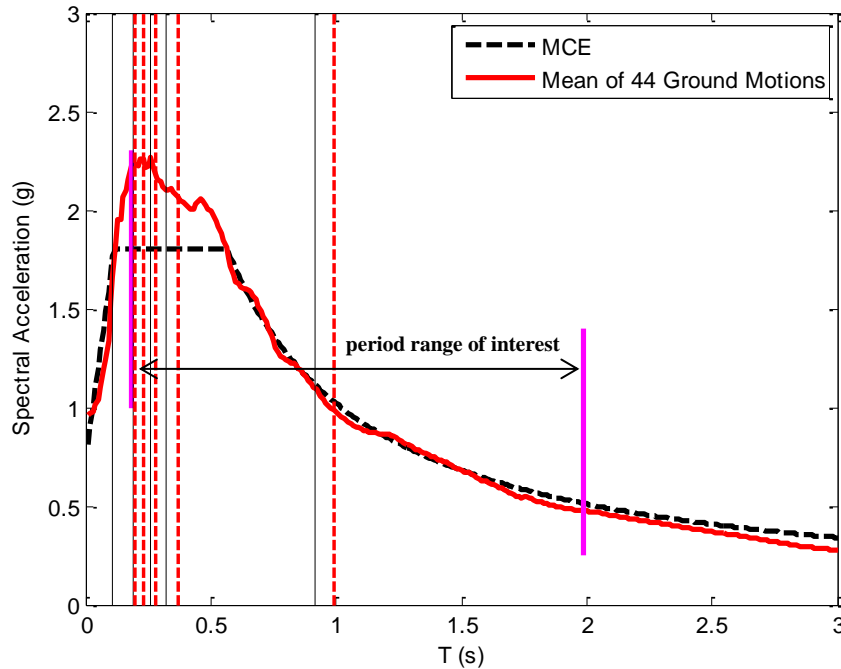

Figure 2. Mean acceleration response spectra of the scaled ground motions under MCE level

RESULTS AND DISCUSSION

Distribution of PFA/PGA

Time-history analyses of the two SCBF models performed using the ground motion suite scaled to DBE and MCE levels produced floor acceleration history. The average PFA normalized by PGA was determined along the normalized height (z/h), i.e. the ratio between the floor height and the total height of the frame. Figure 3 shows the median and 84th percentile values of PFA/PGA and peak interstorey drift ratio (IDR) at each floor of the chevron configuration under DBE and MCE levels.

Figure 4 shows the corresponding distributions for the two-storey X braced frame. In Figures 3 and 4, the floor indexing follows the North American convention where the ground level corresponds to floor 1; 'r' denotes the roof level. It can be seen that the peak IDR increases when the ground motion intensity is increased, while the PFA/PGA ratio generally reduces as the intensity of the earthquake is increased. Due to the complicated behaviour of the braces in the SCBF systems, the distribution of the acceleration is different based on the location of concentrated nonlinearity. For instance, inelastic deformation concentrates in the beam of the sixth floor in the two-storey X structure, which results in PFA/PGA reduction and a large interstorey drift at the sixth floor. As can be seen in the profiles of PFA/PGA, the lowest values are observed in the fifth and sixth floors of the two-storey X structures, as these floors undergo the largest interstorey drifts. In the case of the chevron configuration, the lowest PFA/PGA occurs in the sixth floor, which has the largest interstorey drift. Because of the unsymmetrical behaviour of the braces under tension and compression, the hysteresis behaviour substantially deteriorates and makes the prediction of the nonlinear behaviour quite complicated.
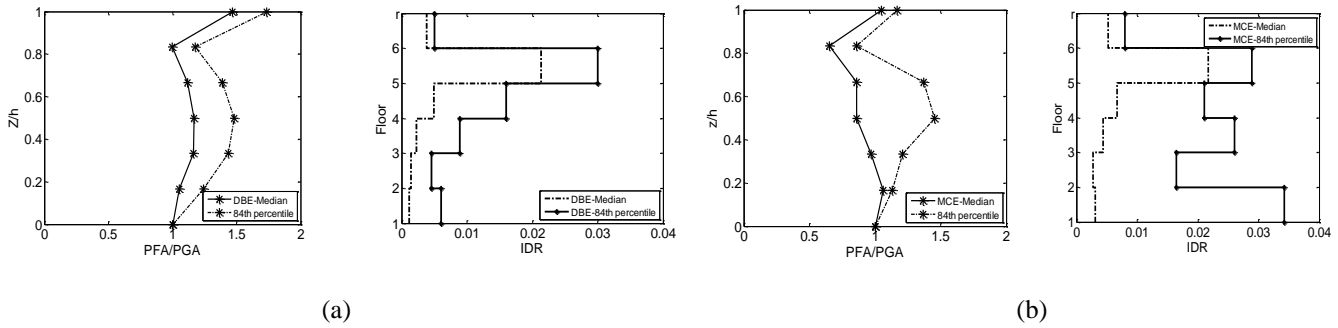

(a)   (b)

Figure 3. Distribution of PFA/PGA and peak IDR of the chevron configuration under (a) DBE (b) MCE

(a)   (b)
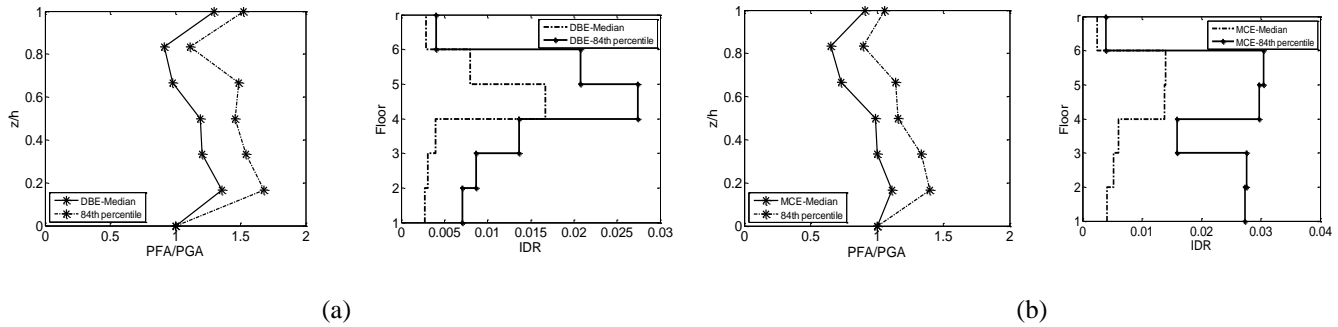
Figure 4. Distribution of PFA/PGA and peak IDR of the two-storey X configuration under (a) DBE (b) MCE

An important step toward computing the seismic forces on attached NSCs involves estimating the acceleration at their attachment points. The ASCE 7-16 code provisions for NSCs require that the horizontal seismic design force on the component is computed from the PFA, modified by appropriate factors to account for the component's importance, dynamic amplification, and response modification representing the energy absorption capability of the component and its attachments [6]. The PFA is assumed to be equal to the PGA (which is assumed to be 40% of the spectral acceleration at 0.2 s at the building site) times the so-called height factor, which is assumed to vary linearly from 1 at the ground level to 3 at the roof, i.e. $1 + 2 z/h$. The effect of the lateral load-resisting system and the dynamic characteristics of the building, including the fundamental period, are neglected in the current code formula.

Figure 5 shows the PFA/PGA values from the analyses of both SCBF systems at the DBE level. As can be seen from a large portion of the data points, yielding of the braces limits the transmitted accelerations along the height, making the height factor formula in the code gradually overconservative with increasing z/h. Figure 6 shows the median and 84th percentile curves corresponding to the DBE data. Considering the mean plus one standard deviation, the ASCE 7-16 formula overestimates the height factor at all levels but the first.

Instead of a linear relationship, the height factor can be represented by a nonlinear relationship of the form:

$$\frac{\text{PFA}}{\text{PGA}} = 1 + \alpha \left(\frac{z}{h}\right)^{\beta} \tag{1}$$
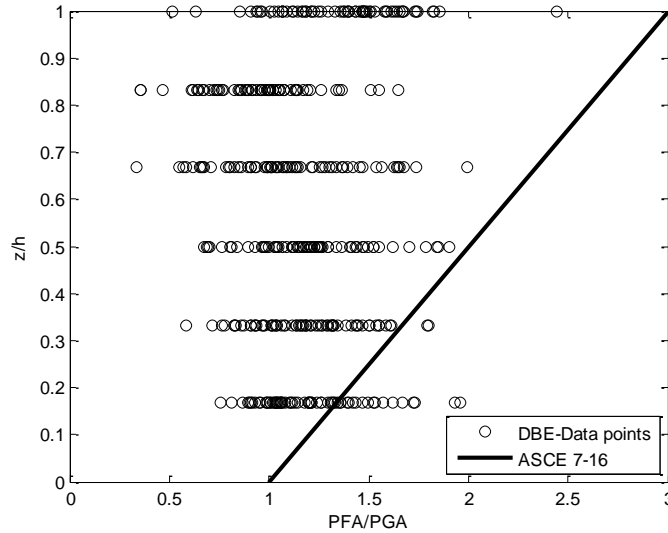

Figure 5. PFA/PGA versus z/h data points from the time history analyses at the DBE level, compared against the assumed linear distribution in ASCE 7-16 and NBC 2015

where α and β can be obtained from nonlinear regression. For $\alpha = 2$ and $\beta = 1$, Equation (1) represents the ASCE 7-16 formula for the height factor. Figure 6 shows the fitted curve through the 84th percentile data points corresponding to Equation (1) with $\alpha = 0.472$ and $\beta = 0.215$. The resulting acceleration profile over the height for the modelled midrise building with two possible SCBF configurations is considerably different from that assumed in the code.
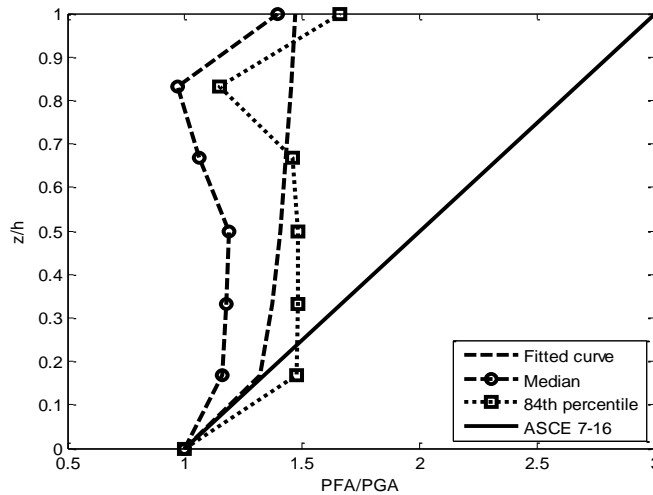

Figure 6. Height factor variation (DBE level)

Floor Response Spectra

The absolute floor acceleration time history obtained from the response analysis of the OpenSees models are used to develop elastic Floor Response Spectra (FRS). Figures 7 and 8 show the 5% and 2% damped mean FRS, respectively, for different storeys of the chevron and two-storey X systems corresponding to the 44 ground motions scaled to DBE level. Although a damping of 5% has been typically considered for NSCs, the limited information in the literature suggests that values in the 1-

3% range are more appropriate for typical NSCs [17]. The first four modal periods of the systems are depicted on the figures using vertical dashed lines. As can be seen, the floor spectra exhibit large peaks around the higher-mode periods. This is consistent with Figure 2 (in which the vertical lines show the modal periods of the chevron and two-storey X systems) where it can be seen that the ground motions contain considerable energy at the higher modes of the structures. This is significant considering that most NSCs in typical buildings have fundamental periods that lie in the short-period range (e.g. < 0.5 s).

According to Figures 7 and 8, the peaks of the floor spectra near the first structural period (0.9~1.0 s) increase along the height of the frames. This means that attached NSCs in this period range (which are less common) will experience demands that follow an increasing trend with height, as is suggested by the height factor formula in ASCE 7-16 [6] and NBC 2015 [7]. However, the floor spectral accelerations are lower in the higher modes for the floors with more inelasticity. For instance, the FRS for the sixth floor reduces around the second and third modes, while it increases around the fourth mode. The results imply that there is no easily discernible trend between the concentration of nonlinearity and the amplification of the acceleration in higher modes, as was also observed by Ray-Chaudhuri and Hutchinson [18]. As noted earlier, it is in this period range that most NSCs reside.
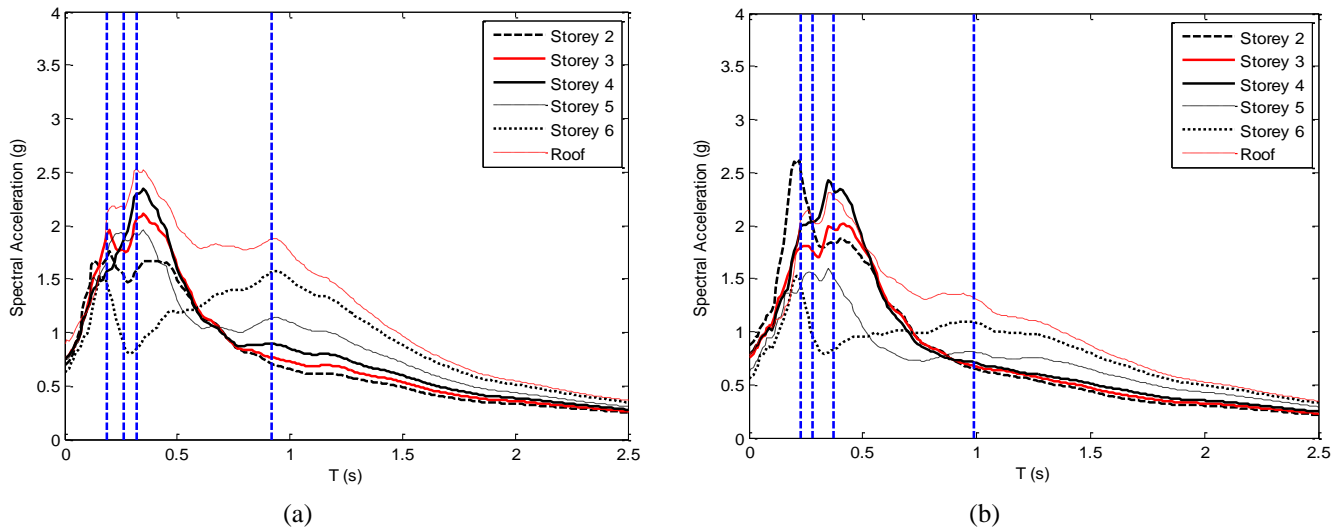

(a)   (b)

Figure 7. Floor response spectra for NSCs with 5% damping ratio under DBE: (a) Chevron (b) Two-storey X
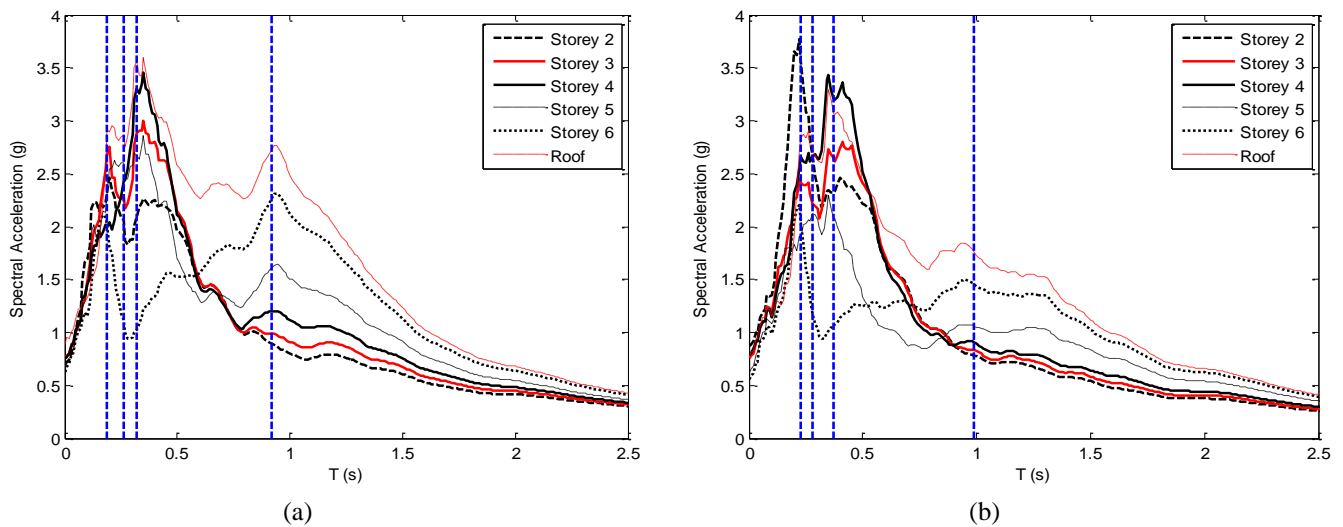

(a)   (b)

Figure 8. Floor response spectra for NSCs with 2% damping ratio under DBE: (a) Chevron (b) Two-storey X

Component Amplification Factor

The ratio of the Peak Component Acceleration (PCA) and the PFA is known as the component amplification factor, a_p in ASCE 7-16 [6]. The value of a_p varies from 1.0 to 2.5, depending on the period of the component (T_p) relative to the structure's fundamental period (T_{B1}). Although the current guidance in the commentary of ASCE 7-16 considers only the fundamental period of the structure for determining a_p, this might be misguided, even for midrise structures, considering observations on the dominating effect of higher modes on the spectral demands on most acceleration-sensitive NSCs. Since the vibrational characteristics of the structure may not be known at the time the NSCs are ordered, seismic design codes recommend that a value of 2.5, i.e. the maximum, be assigned to NSCs that are commonly considered flexible [6]. While this factor is considered to be constant over a wide period range of NSCs, Figure 9 shows that the mean FRS normalized by the PFA is larger than $a_p = 2.5$ at several floors over a period range that covers a significant portion of the acceleration-sensitive NSC stock. For example, considering that the fundamental period of both SCBF systems is between $T_{B1} = 0.9$ s and $T_{B1} = 1.0$ s (Table 1), Figure 9 shows a component amplification factor upwards of 3 for T_p / T_{B1} between 0.25 and 0.5, while ASCE 7-16 [6] recommends taking $a_p = 1.0$ in this period range.

Furthermore, the results demonstrate that the amplification factor of a component depends not only on the fundamental periods of the component and of the structure, but also on the location of the component and the distribution of nonlinearity in the structure. Based on the IDR profiles shown in Figures 3 and 4, concentration of inelastic deformations resulted in larger drifts and smaller normalized accelerations in the corresponding floors. This is also reflected in Figure 9, where yielding in the sixth floor resulted in lower values of the component amplification factor for T_p / T_{B1} between 0.25 and 0.5.
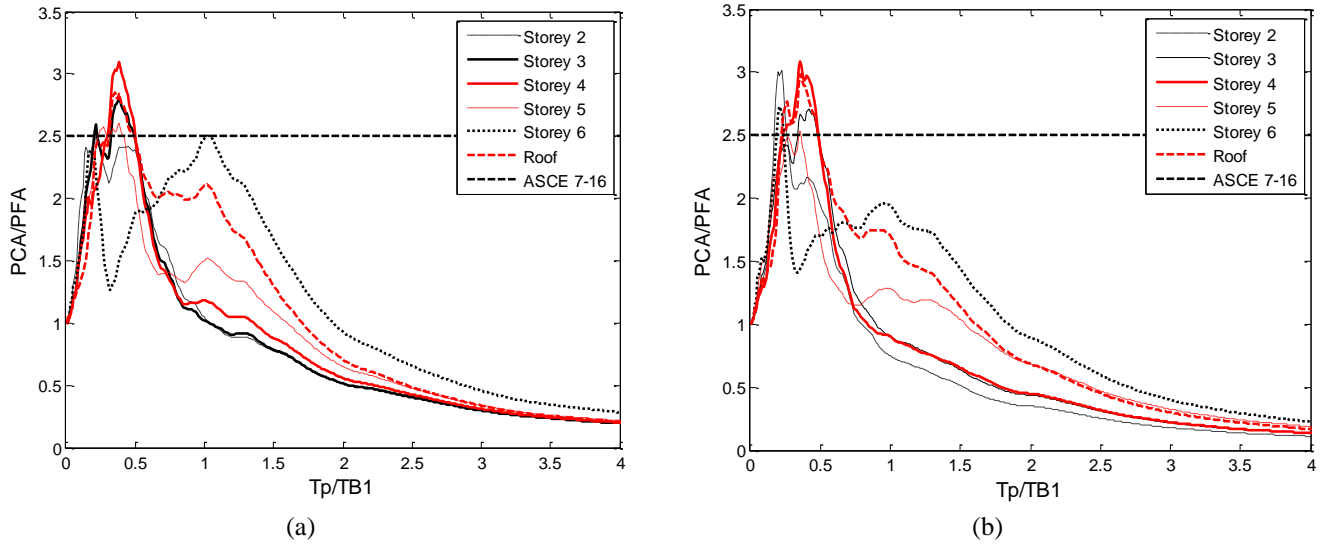

Figure 9. Component amplification factor for the (a) chevron and (b) two-storey X configurations with 5% damping ratio of NSC

CONCLUSIONS

This study investigated the acceleration demands on nonstructural components (NSCs) in two 6-storey office building archetypes on Site Class D in San Francisco. Two special concentrically braced frame configurations were considered (a chevron and a two-storey X) for the lateral load-resisting system. The contribution of the gravity framing system was also considered. Nonlinear response history analysis of the two systems was carried out using the FEMA P-695 [16] suite of 44 ground motions, scaled to the DBE and MCE intensity levels. The main findings of the study can be summarized as follows:

• The distributed nonlinearity of the structural system resulted in a reduction in peak floor accelerations (PFAs). This allows smaller forces for the design of rigid NSCs and their attachments.

• The height factor formula (which gives the variation PFA/PGA over the height of the structure) in the current seismic design code criteria for NSCs was shown to provide overconservative values in most floors levels of the midrise building considered. The results of the analyses were used to propose a revised height factor formula that varies nonlinearly.

• The shape of the floor response spectra is considerably affected by the location of the NSCs, stiffness distribution of the structure in the nonlinear range, the damping ratio of the NSCs and the modal periods.

• Considering the role of higher mode resonance in the floor response spectra of yielding structures results in different component amplification factors of NSCs relative to what is provided in ASCE 7-16.

ACKNOWLEDGEMENTS

REFERENCES

[1] Taghavi, S., Miranda, E. (2003). "*Response assessment of nonstructural building elements*". Report No. PEER 2003/05. Pacific Earthquake Engineering Research Center, Richmond, CA.

[2] Filiatrault, A., Sullivan, T. (2014). "Performance-based seismic design of nonstructural building components: The next frontier of earthquake engineering". *Earthquake Engineering and Engineering Vibration*, 13(1), 17-46.

[3] Anajafi, H., Medina, R. (2018). "Lessons learned from evaluating the response of instrumented buildings in the US: The Effect of Supporting Building Characteristics on Floor Response Spectra". *Earthquake Spectra*. https://doi.org/10.1193/081017EQS159M.

[4] Anajafi, H., Medina, R. (2018). "Evaluation of ASCE 7 equations for designing acceleration sensitive nonstructural components using data from instrumented buildings". *Earthquake Engineering and Structural Dynamics*, 47(4), 1075-1094.

[5] Miranda, E., Vamvatsikos, D., Kazantzi, A. (2018). "*New approach to the design of acceleration-sensitive non-structural elements in buildings*". In 16th European Conference on Earthquake Engineering. Thessaloniki, Greece.

[6] ASCE (2016). American Society of Civil Engineers. "*Minimum design loads for buildings and other structures*". ASCE/SEI 7‑16, Reston, Va., 2016.

[7] NBC. (2015). National Building Code of Canada. Institute for Research in Construction, National Research Council of Canada, Ottawa, Ont.

[8] Fathali, S., Lizundia, S.E. (2011). "Evaluation of current seismic design equation for nonstructural components in tall buildings using strong motion records". *The Structural Design of Tall and Special Buildings,* 20, 30-46.

[9] Kehoe, B.E., Freeman, S.A. (1998). "*A critique of procedures for calculating seismic design forces for nonstructural elements*". Seminar on Seismic Design, Retrofit, and Performance of Nonstructural Components, ATC-29-1, Applied Technology Council, Redwood City, California.

[10] Searer, G.R., Freeman, S.A. (2002). "*Unintended consequences of code modification*". Proceeding. 7th U.S. National Conference on Earthquake Engineering, EERI, Boston, Massachusetts, CD-Rom.

[11] NIST (2010). "*Evaluation of the FEMA P-695 Methodology for quantification of building seismic performance factors*". GCR 10-917-8. Prepared by the Applied Technology Council for the National Institute of Standards and Technology, Gaithersburg, MD.

[12] AISC, (2016). "*Seismic provisions for structural steel buildings*". ANSI/AISC 341-16, American Institute for Steel Construction, Chicago, Illinois.

[13] AISC, (2016). "*Prequalified connections for special and intermediate steel moment frames for seismic applications*". ANSI/AISC 360-16, American Institute for Steel Construction, Chicago, Illinois.

[14] Pacific Earthquake Engineering Research Center (PEER), (2009). OpenSees (Open System for Earthquake Engineering Simulation), developed by PEER, University of California, Berkeley, California, http://opensees.berkeley.edu/.

[15] Uriz, P., Filippou, F.C., Mahin, S.A. (2008). "Model for cyclic inelastic buckling of steel braces". *Journal of Structural Engineering*, 134(4):619‑628.

[16] FEMA, (2009). "*Quantification of building seismic performance factors*". FEMA P-695, prepared by Applied Technology Council for the Federal Emergency Management Agency, Washington, D.C.

[17] Kazantzi, A., Vamvatsikos, D., Miranda, E. (2018). "*Effect of yielding on the seismic demands of nonstructural elements*". 16th European conference on Earthquake Engineering. Thessaloniki, Greece.

[18] Ray-Chaudhuri, S., Hutchinson, T.C. (2011). "Effect of nonlinearity of frame buildings on peak horizontal floor acceleration". *Journal of Earthquake Engineering,* 15(1):124-142.